

UniHead: Unifying Multi-Perception for Detection Heads

Hantao Zhou, Rui Yang, Yachao Zhang, Haoran Duan, Yawen Huang, Runze Hu, Xiu Li, Yefeng Zheng, *Fellow, IEEE*

Abstract—The detection head constitutes a pivotal component within object detectors, tasked with executing both classification and localization functions. Regrettably, the commonly used parallel head often lacks omni-perceptual capabilities, such as deformation perception, global perception and cross-task perception. Despite numerous methods attempt to enhance these abilities from a single aspect, achieving a comprehensive and unified solution remains a significant challenge. In response to this challenge, we have developed an innovative detection head, termed UniHead, to unify three perceptual abilities simultaneously. More precisely, our approach (1) introduces deformation perception, enabling the model to adaptively sample object features; (2) proposes a Dual-axial Aggregation Transformer (DAT) to adeptly model long-range dependencies, thereby achieving global perception; and (3) devises a Cross-task Interaction Transformer (CIT) that facilitates interaction between the classification and localization branches, thus aligning the two tasks. As a plug-and-play method, the proposed UniHead can be conveniently integrated with existing detectors. Extensive experiments on the COCO dataset demonstrate that our UniHead can bring significant improvements to many detectors. For instance, the UniHead can obtain +2.7 AP gains in RetinaNet, +2.9 AP gains in FreeAnchor, and +2.1 AP gains in GFL. The code will be publicly available.

Index Terms—Detection head, Unifying multi-perception, Transformer, Object detection.

I. INTRODUCTION

Object detection is a fundamental but challenging task that aims to locate and recognize objects of interest in images. Recent years have witnessed remarkable progress in object detection, with advancements in backbone design [1]–[3], feature fusion network optimization [3]–[6], and effective training strategies [7]–[12]. Despite these impressive breakthroughs, the crucial role of detection heads in object detection has not been fully explored in existing research.

The primary purpose of detection heads is to perform accurate classification and localization tasks by utilizing the intricate features extracted from the backbone. One prevalent approach is the parallel head [7], [9], [13], which establishes two isolate branches by employing stacked convolutions to learn task-relevant features, as depicted in Fig. 1(a). However,

Hantao Zhou, Rui Yang, Yachao Zhang, Xiu Li are with Tsinghua Shenzhen International Graduate School, Tsinghua University, Shenzhen, 518055, China (e-mail: hantaozh@outlook.com, r-yang20@mails.tsinghua.edu.cn, yachaozhang@std.xmu.edu.cn, li.xiu@sz.tsinghua.edu.cn).

Runze Hu is with the School of Information and Electronics, Beijing Institute of Technology, Beijing, 100086, China (e-mail: hrzlpk2015@gmail.com).

Haoran Duan is with the Department of Computer Science, Durham University (E-mail: haoran.duan@ieee.org).

Yawen Huang and Yefeng Zheng are with Tencent Jarvis Lab, Shenzhen, China (E-mail: yawenhuang@tencent.com; yefengzheng@tencent.com).

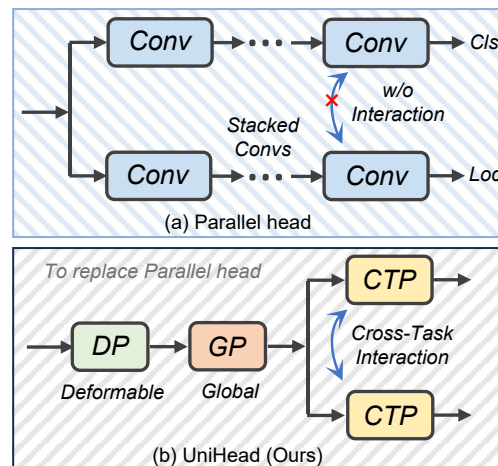


Fig. 1. Overview of the parallel head (a) and our UniHead (b). UniHead integrates *deformation perception* (DP), *global perception* (GP), and *cross-task perception* (CTP) in the detection head.

despite its widespread use, this approach has several limitations, especially the lack of perceptual capabilities necessary for an ideal detector.

In concrete, an ideal detector should possess three critical perceptual capabilities: *deformation perception*, *global perception*, and *cross-task perception*. Specifically, natural objects exhibit two types of diversities: geometric deformation diversity, scale and shape diversity. The former requires the detector can adaptively sample object-relevant features to counter the geometric deformation of the target object (*deformation perception*), while the latter requires *global perception* to capture global features and model long-range dependencies. Additionally, many works [8], [14], [15] have observed that classification predictions and localization predictions may be misaligned, *i.e.*, boxes with high classification scores cannot always be accurately localized. Therefore, the detection head necessitates *cross-task perception* to comprehensively integrate the supervision information from both tasks, thus resulting in consistent detection for classification and localization.

However, the commonly used parallel head [7], [9], [13] cannot provide these perceptions stemming from the convolution properties and the parallel structures. Particularly, the convolution mechanism is limited in both deformation and global perception, as it samples the input feature map at fixed local locations. The parallel structures perform two tasks independently and lack cross-task perception to execute interaction between them, as shown in Fig. 1(a).

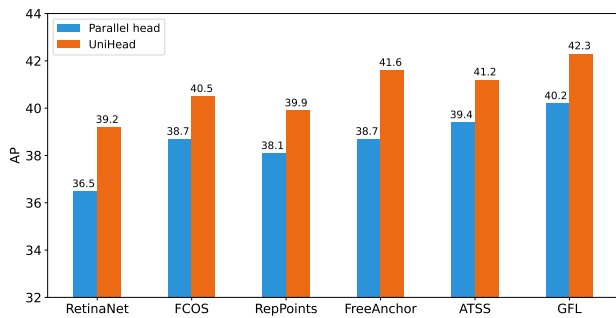


Fig. 2. Our UniHead significantly improves the performance of different detectors, including anchor-based (RetinaNet [7]), anchor-free center-based (FCOS [13]), anchor-free keypoint-based (Reppoints [16]) and strong baseline (FreeAnchor [17], ATSS [9], GFL [8]).

Recently, researchers have sought to mitigate the aforementioned issues by proposing novel detection heads. For instance, the dynamic head [18] integrates multiple attentions to unify scale-awareness and spatial-awareness, which alleviates the locality bias of the convolution mechanism. GFL [8] and TOOD [14] combine the supervision information (*e.g.*, classification score and IOU) from both tasks to improve the model’s ability in cross-task perception, thus achieving consistent detection prediction. Nonetheless, existing approaches are inclined towards enhancing only one of the three perception aspects, lacking a unified approach that can collectively enhance all of these perceptions simultaneously.

In this paper, we thereby propose a plug-and-play detection head, dubbed *UniHead*, to address the above problems from a comprehensive and integrated perspective. UniHead involves different modules to imbue the detector with a comprehensive perceptual capability while not imposing additional computational or architectural burdens. The overall framework of UniHead is presented in Fig. 1(b).

Specifically, we first introduce the deformation perception to UniHead by the classical deformable convolution [19]. This allows the model to sample spatial locations away from local and fixed shapes, resulting in a more effective perception of deformed objects. Second, we propose a Dual-axial Aggregation Transformer (DAT) to model long-range dependencies effectively. DAT performs self-attention on the horizontal and vertical axes in parallel in the channel-compressed space. This design empowers it to capture global information within a single module while maintaining low computational complexity. More importantly, we introduce a Cross-task Interaction Transformer (CIT), which uses cross-attention to facilitate interaction between the classification and localization tasks. By incorporating CIT, UniHead can not only capture the abundant context of one task but also leverage relevant context from the other task, thus explicitly promoting mutual alignment between the two tasks.

Based on the above three meticulously designed modules, UniHead can effectively enhance multiple perceptual abilities. Our UniHead can be conveniently integrated with existing detectors with ease as a plugin. We conduct extensive experiments on the MS-COCO [20] benchmark to demonstrate the effectiveness of our approach. As shown in Fig. 2, UniHead

consistently improves the performance of classical detectors by a large margin. Specifically, when applying UniHead to RetinaNet [7] with ResNet-50 [1] as the backbone, it achieves 39.2 AP and considerably improves the RetinaNet baseline by 2.7 AP. With powerful backbone Swin-B [21] pre-trained on ImageNet-22K dataset [22], our Unihead achieves 54.3 AP, demonstrating the potential of our approach and compatibility with large models. The main contributions of this work can be summarized as follows:

- We propose a novel detection head, namely UniHead, which improves the detection performance by jointly enhancing three essential perceptual abilities of a detector, *i.e.*, deformation perception, global perception and cross-task perception.
- We devise a Dual-axial Aggregation Transformer (DAT) to capture global features effectively and efficiently. Additionally, we introduce a Cross-task Interaction Transformer (CIT) meticulously crafted to facilitate interactions between the classification and localization tasks.
- We have verified various detectors equipped with our method on the MS-COCO benchmark, and results show that our method can constantly improve these detectors by 1.7 \sim 2.9 AP with even fewer computational costs.

II. RELATED WORK

A. Object Detection

Recent years have witnessed flourished developments in object detection [7], [23], [24], with two main categories of object detectors: two-stage and one-stage detectors. Two-stage detectors, such as the R-CNN series [25]–[28], generate region proposals using a Region Proposal Network (RPN) in the first stage and then refine the predictions of these proposals in the second stage. Different from the two-stage paradigm, one-stage detectors eliminate the region proposal step and instead classify and regress the bounding box directly. However, earlier one-stage detectors trailed the detection performance until the emergence of RetinaNet [7], which involves focal loss to solve the class imbalance problem. Following RetinaNet, various detectors eliminate the widely-used anchor and develop anchor-free detectors, which use center [13] and corner points [16] to represent objects. Some researchers also propose novel loss [8] and training strategies [9] to improve the performance of detectors.

B. Detection Head

The detection head constitutes a pivotal element of a detector, with the widely adopted parallel head being the default choice. However, recent research has unveiled that this standard detection head falls short of achieving optimal detection performance. For instance, Double-Head [15] suggests that a fully connected head is more suitable for classification tasks, whereas a convolution head is better suited for localization tasks. GFL [8] has enriched the concept of a detection head by introducing soft labels. It leverages the IOU score from the localization task as the classification label, forming a joint representation of localization quality and classification. TOOD [14] has devised a task-aligned head, designed to

strengthen the interaction between classification and localization tasks. Dynamic Head [18] employs attention mechanisms to augment the detection head’s perceptual capabilities concerning scale and spatiality. Despite these commendable advancements, current methods tend to address specific sub-problems individually. This paper introduces a comprehensive detection head that enhances the model’s detection capabilities from multiple perspectives.

C. Attention Mechanism

Attention mechanisms hold a critical role in human perception. Inspired by this, they are also widely used in deep learning to further boost the performance of the model [29]–[32]. Among various attention mechanisms, deformable convolution [19] can be perceived as a special attention mechanism, which adds a learnable offset to the vanilla convolution to sample spatial locations away from local regions. In recent times, Transformers have garnered substantial acclaim in the domain of computer vision, primarily due to their prowess in modeling long-range dependencies [21], [33]–[36]. Although Transformer can provide a global receptive field for the model, its complexity is quadratic with the image resolution, which limits its application to high-resolution downstream tasks (including object detection). Therefore, plenty of algorithms have been proposed to ameliorate this problem, including introducing global token [37], [38], reducing the spatial size of attention [39], [40], designing novel attention mechanisms (e.g., local-windows attention [21], axial attention [41], criss-cross attention [42], cross-shaped window attention [43]). In this article, we harness existing attention mechanisms or devise novel ones to augment perceptual capabilities. In order to minimize the computational overhead, we have also incorporated lightweight designs, resulting in our UniHead being both effective and efficient.

III. UNIHEAD

The widely used parallel head [7], [9], [13] fails to effectively cope with two properties of detection tasks: the diversity of objects in nature as well as the interaction between classification and localization, due to the limitations of convolution and parallel structures. To ameliorate this issue, we propose a novel detection head, termed UniHead, as shown in Fig. 1(b).

UniHead can provide three capabilities for the model: *deformation perception*, *global perception* and *cross-task perception*, in a unified form.

- **Deformation Perception.** Deformation Perception enables the model to learn object-related features adaptively, instead of being trapped in fixed windows and local locations.
- **Global Perception.** Global Perception allows the model to perceive global features and model long-range dependencies, thus detecting objects with various scales more accurately.
- **Cross-Task Perception.** Cross-Task Perception can perform interaction between two tasks to introduce additional supervision information for each task, leading to more consistent prediction.

We leverage or introduce dedicatedly designed modules to achieve these perceptions and unifying them to build our UniHead. In general, given a multi-scale feature map, the UniHead executes these three modules to catch three perception features. Then, the output features are employed to perform classification and localization. With this framework, UniHead attempts to unify the three perceptual capabilities in a single head. In the following, we delineate the three perceptions in detail.

A. Deformation Perception

The objects in natural scenes are complex, with various contents and geometric transformations. The vanilla convolution with a fixed kernel (e.g., 3×3) fails to tackle this challenging situation well. Thus, inspired by [44], we introduce deformation perception (DP) into the UniHead by using deformable convolution. Deformable convolution can perceive object transformations through learned offsets and scales on multi-scale features. Given a 3×3 kernel and offsets $p_k \in \{(-1, -1), (-1, 0), \dots, (1, 1)\}$, the deformation learning process at the location p can be expressed as:

$$X^{DP}(p) = \sum_{k=1}^K W_k \cdot B(X; p + p_k + \Delta p_k) \Delta m_k, \quad (1)$$

where $K = 9$ donates the number of sampling locations for one 3×3 convolution operation and W_k represents the convolution weights of the k -th sampling location. $B(\cdot; \cdot)$ refers to bilinear interpolation on the feature X . Δp_k and Δm_k denote the predicted offsets and scales at the k -th sampling location, respectively. The predicted offsets make feature sampling not be restricted to a fixed location, and the modulation scales regulate the importance of each sampling location. With these adaptive sampling offsets and modulation scales, we introduces deformable representation capabilities into the model, thus facilitating the detection of objects with complex shapes and diverse appearances.

B. Global Perception

Objects with varying scales and shapes often exist in the image, which requires the detector to capture global features to locate their complex boundaries. To address this issue, we propose a Dual-axial Aggregation Transformer (DAT) to model long-range dependencies, resulting in global perception enhancement to detectors. The DAT involves two parts: efficient dual-axial attention and cross-axis aggregation block.

Efficient Dual-axial Attention. Although Transformer has demonstrated its effectiveness in global modeling capabilities, its overwhelming computational burden limits its wider range of application. Alternative methods, such as local window attention [21] and spatial reduction operation [34], [39], [40], often forsake the global capability or lose some spatial information. To overcome these limitations, we propose an Efficient Dual-axial Attention (EDA).

As shown in Fig. 3(a), the EDA utilizes horizontal and vertical axial attention in parallel to model long-range dependencies. For horizontal axial attention, the input feature

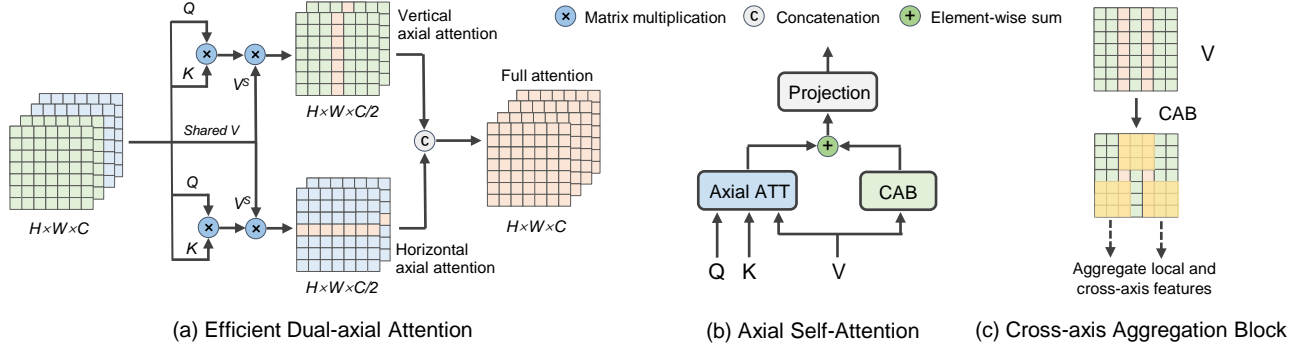


Fig. 3. Illustration of our Dual-axial Aggregation Transformer (DAT). ATT and CAB represent attention and Cross-axis Aggregation Block, respectively.

$X \in \mathbb{R}^{H \times W \times C}$ is evenly split into H non-overlapping horizontal axial stripes, each with W tokens. Let $X_i \in \mathbb{R}^{W \times C}$ denotes the i -th stripe, and the self-attention of X_i can be formulated as:

$$(Q_i, K_i, V_i^S) = (X_i W_Q, X_i W_K, X_i W_V^S),$$

$$\hat{Y}_i = \text{Attention}(Q_i, K_i, V_i^S) = \text{Softmax}\left(\frac{Q_i K_i^T}{\sqrt{d_k}}\right) V_i^S, \quad (2)$$

where $W_Q \in \mathbb{R}^{C \times \frac{C}{2}}$, $W_K \in \mathbb{R}^{C \times \frac{C}{2}}$, $W_V^S \in \mathbb{R}^{C \times \frac{C}{2}}$ represent the projection matrices of queries, keys and values on the input X_i . Note that channel reduction operation is utilized when calculating queries, keys and values, thus making the attention perform in the channel-compressed space. V_i^S and W_V^S represent the shared values and projection matrix and will be used in both horizontal and vertical axial attention. d_k is the dimension of K_i . $\hat{Y}_i \in \mathbb{R}^{W \times C}$ is the horizontal attention output of X_i . The vertical axial self-attention can be similarly derived and its output is denoted as \tilde{Y} . Finally, the outputs of two parts are concatenated along the channel dimension. The process is formulated as:

$$\text{EDA}(X) = \text{Cat}(\hat{Y}, \tilde{Y}) W_O, \quad (3)$$

where Cat denotes the channel-wise concatenation; $W_O \in \mathbb{R}^{C \times C}$ is the commonly used projection matrix for feature fusion. The complexity of EDA is:

$$\Omega(\text{EDA}) = HWC \times (3.5C + H + W). \quad (4)$$

Thus, the EDA reduces the complexity of attention to be quadratic to image height or width ($O(H^2)$ or $O(W^2)$), rather than to the image resolution ($O((HW)^2)$).

Compared with previous axial strip-like self-attention [41], [43], our EDA is computed in the channel compressed space and shares the same value map. These two operations enable our EDA to capture global features in a single module more efficiently. Ablation experiments (Table VI) demonstrate that the proposed attention can bring better performance.

Cross-axis Aggregation Block. Although the EDA can effectively model long-range dependencies between tokens, it falls short in learning local information due to the lack of inductive bias of self-attention. In addition, axial attention cannot aggregate cross-axis information directly. In order to complement the EDA with the locality and achieve global

and local coupling, we propose a cross-axis aggregation block (CAB). As illustrated in Fig. 3(b), the CAB is applied on the value (V) map and operates in parallel to the axial attention. Formulaically, this process can be expressed as:

$$\hat{Z} = \hat{Y} + \text{CAB}(\hat{V}), \quad (5)$$

where \hat{V} and \hat{Z} denote the value map and output of horizontal axial attention, respectively. The function of CAB can be easily implemented by a 3×3 depth-wise convolution. CAB offers a more flexible mechanism that not only provides attention with positional information but also enables interaction and aggregation among different axial stripe-like attentions, as depicted in Fig. 3(c).

With the proposed EDA and CAB, our Dual-axial Aggregation Transformer (DAT) can effectively model long-range dependencies, achieve global perception, and thus perform more precise localization.

C. Cross-Task Perception

Object detection is the integration of classification and localization. The detection head is required to utilize information from both tasks to make consistent predictions, rather than executing the two tasks independently. Namely, the detector is required to output the box with precise location and high classification confidence. Thus, we propose a Cross-task Interaction Transformer (CIT) that compensates for the model's ability to perform cross-task interaction. As shown in Fig. 4, the CIT possesses two significant components: cross-task channel-wise attention and locality enhancement block.

Cross-task Channel-wise Attention. We leverage channel-wise cross-attention to perform interaction between classification and localization tasks. Channel-wise attention can benefit the model from two aspects: (1) reduce the complexity of attention to be linear with the image size; (2) enhance the channel-wise global perception for the model while being complementary with DAT that focuses on global spatial-wise perception. And the cross-attention empowers the model to leverage features from one task to inform and guide the feature learning process of another task.

Specifically, prior to feeding features into CIT, we first utilize conditional positional encoding [45] to encode position information for classification and localization features, and the

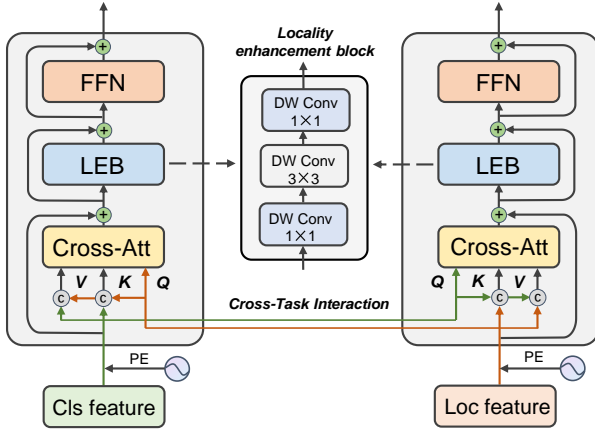


Fig. 4. Illustration of the proposed Cross-task Interaction Transformer. PE denotes the positional encoding process.

outputs denote $X^c \in \mathbb{R}^{(H \times W) \times C}$ and $X^l \in \mathbb{R}^{(H \times W) \times C}$, respectively. As shown in the left side of Fig. 4, when CIT is applied to the classification branch, the Cross-task Channel-wise Attention (CCA) can be described as:

$$\begin{aligned} (K^c, V^c) &= (X^c W_K^c, X^c W_V^c), \\ (K^l, V^l) &= (X^l W_K^l, X^l W_V^l), \\ Q &= X^l W_Q^l, K = \text{Cat}(K^c, K^l), V = \text{Cat}(V^c, V^l), \\ \text{CCA}(X^c, X^l) &= \text{CA}(Q, K, V) = V \text{Softmax}\left(\frac{Q^T K}{\sqrt{d_k}}\right), \end{aligned} \quad (6)$$

where W_K^c, W_V^c, W_K^l and $W_V^l \in \mathbb{R}^{C \times \frac{C}{2}}$ are the projection matrices of keys and values for the input X^c and X^l , respectively; $W_Q^l \in \mathbb{R}^{C \times C}$ denotes the projection matrix of queries for the input X^l ; CA represents the channel-wise attention that calculates attention among channels.

As shown in Equation 6, we use the cross-task supervision information from X^l as queries to guide the representation learning of classification feature X^c . Furthermore, we concatenate the features of two tasks to generate keys and values, thus further fusing cross-task information. Ablation experiments show (Table IX) that the attention with cross-task information interaction can achieve superior performance, without adding any parameter and computation.

Locality Enhancement Block. Since channel-wise attention lacks the ability to learn local spatial-wise features, we propose a locality enhancement block (LEB) to alleviate this problem. The LEB is lightweight and effective, which builds on depth-wise convolutions with different kernel sizes. Formulaically, it can be described as:

$$\text{LEB}(X^{\text{CCA}}) = DW_{1 \times 1}(DW_{3 \times 3}(DW_{1 \times 1}(X^{\text{CCA}}))), \quad (7)$$

where DW denotes the depth-wise convolution; X^{CCA} represents the features output from cross-task channel-wise attention (CCA). The two 1×1 depth-wise convolutions can further modulate the importance of each channel, which are channel-wise scales. The 3×3 depth-wise convolution can learn locality information and compensate inductive bias for the model.

So far, three perception modules have been illustrated in detail. These modules are connected in series to form our UniHead, which can obtain absolute gains on both object detection (Table I) and instance segmentation (Table XI) tasks.

IV. EXPERIMENTS

A. Dataset and Evaluation Metrics

We evaluate our approach on the large-scale detection benchmark MS-COCO 2017 dataset [20]. MS-COCO dataset has 80 object categories of around 160K images, with 118k images for training, 5k images for validation and 41k images for testing. We train our model on *train2017* subset and evaluate the performances on the *val2017* subset for ablation study and on *test-dev* subset for comparison with state-of-the-art methods. The detection performance is measured by the standard COCO Average Precision (AP) metrics. We employ Params and GFLOPs to evaluate the model efficiency, which represent the number of parameters and floating point operations of the model, respectively.

B. Implementation Details

We employ our UniHead as a plugin to replace the default parallel head in different classical detectors. We implement our method based on the popular mmdetection [46] and use the models pretrained on the ImageNet [22] dataset as the backbone. We adopt AdamW as the optimizer with an initial learning rate of 0.0001 and a weight decay of 0.2. A warmup strategy is employed to stabilize the training for the first 500 steps, which is the default strategy in mmdetection. When training 12 epochs, the learning rate decreased by a factor of 0.1 after 9-th and 11-th epochs. All experiments are performed on 8 V100 GPUs each with 32GB memory.

C. Main Results

We first replace the parallel head with our UniHead in different popular detectors to evaluate the effectiveness of our approach. We then integrate the UniHead with a range of different backbones to demonstrate the compatibility and versatility of our method.

Applying to classical detectors. We evaluate the effectiveness and generalization ability of the UniHead by plugging it to popular object detectors, including RetinaNet [7], FCOS [13], RepPoints [16], FreeAnchor [17], ATSS [9] and GFL [8]. These selected detectors represent a wide range of object detection frameworks, including anchor-based, anchor-free center-based, anchor-free keypoint-based and strong baseline (improved version of existing works). To ensure a fair comparison, we used a perception module number configuration of 1, 2, 2 to maintain a comparable complexity to the parallel head. The results are reported in Table I. Note Reppoints has fewer convolutions in the parallel head than the other selected detectors, so the complexity of our method is slightly higher. As shown in Table I, UniHead consistently improves the performance of all detectors by notable margins, such as 2.7 AP improvement on RetianNet and 2.9 AP improvement on FreeAnchor, with even fewer parameters and

TABLE I
RESULTS OF APPLYING UNIHEAD TO DIFFERENT CLASSICAL DETECTORS ON COCO *val*2017.

Detector	Note	#Param.	FLOPs	AP	AP ₅₀	AP ₇₅	AP _S	AP _M	AP _L
<i>Anchor-based</i>									
RetinaNet [7]	baseline	37.74M	239.32G	36.5	55.4	39.1	20.4	40.3	48.1
RetinaNet [7]	UniHead	37.34M	239.12G	39.2 (+2.7)	59.7	41.7	23.6	43.0	51.1
<i>Anchor-free</i>									
FCOS [13]	baseline	32.02M	200.55G	38.7	57.4	41.8	22.9	42.5	50.1
FCOS [13]	UniHead	31.61M	200.31G	40.4 (+1.7)	59.8	43.7	24.7	43.8	52.3
<i>Keypoint-based</i>									
RepPoints [16]	baseline	36.62M	218.07G	38.1	58.7	40.8	22.0	41.9	50.1
RepPoints [16]	UniHead	37.40M	243.02G	39.9 (+1.8)	60.7	42.7	24.0	43.6	53.0
<i>Strong Baseline</i>									
FreeAnchor [17]	baseline	37.74M	239.32G	38.7	57.3	41.5	21.0	42.0	51.3
FreeAnchor [17]	UniHead	37.34M	239.12G	41.6 (+2.9)	61.5	45.0	24.3	45.2	54.8
ATSS [9]	baseline	32.07M	205.30G	39.4	57.6	42.8	23.6	42.9	50.3
ATSS [9]	UniHead	31.66M	205.06G	41.2 (+1.8)	59.9	45.1	25.3	44.9	53.7
GFL [8]	baseline	32.22M	208.39G	40.2	58.4	43.3	23.3	44.0	52.2
GFL [8]	UniHead	31.81M	208.16G	42.3 (+2.1)	61.1	45.6	24.5	46.0	55.3

TABLE II
COMPARISON WITH RESULTS USING DIFFERENT BACKBONES ON COCO *test-dev*. THE RESULTS ARE ARRANGED IN THE INCREASING ORDER OF AP. † REPRESENTS THAT THE MODEL IS PRE-TRAINED ON THE LARGE IMAGENET-22K DATASET.

Method	Backbone	Val/Test	Epochs	AP	AP ₅₀	AP ₇₅	AP _S	AP _M	AP _L	Reference
Cascade R-CNN [28]	ResNet-101	test-dev	36	42.8	62.1	46.3	23.7	45.5	55.2	CVPR18
DAB-DETR [36]	ResNet-101	val	50	43.5	63.9	46.6	23.6	47.3	61.5	ICLR22
ATSS [9]	ResNet-101	test-dev	24	43.6	62.1	47.4	26.1	47.0	53.6	CVPR20
DN-DETR [35]	ResNet-101	val	50	45.2	65.5	48.3	24.1	49.1	65.1	CVPR22
RepPoints v2 [47]	ResNet-101	test-dev	24	46.0	65.3	49.5	27.4	48.9	57.3	NeurIPS20
GFLV2 [48]	ResNet-101	test-dev	24	46.2	64.3	50.5	27.8	49.9	57.0	CVPR21
DyHead [18]	ResNet-101	test-dev	24	46.5	64.5	50.7	28.3	50.3	57.5	CVPR21
TOOD [14]	ResNet-101	test-dev	24	46.7	64.6	50.7	28.9	49.6	57.0	ICCV21
UniHead	ResNet-101	test-dev	24	47.7	66.3	52.1	28.9	51.2	59.0	-
ATSS [9]	ResNeXt-101-64x4d	test-dev	24	45.6	64.6	49.7	28.5	48.9	55.6	CVPR20
Sparse R-CNN [49]	ResNeXt-101-64x4d	test-dev	36	46.9	66.3	51.2	28.6	49.2	58.7	CVPR21
HTC [50]	ResNeXt-101-64x4d	test-dev	20	47.1	63.9	44.7	22.8	43.9	54.6	CVPR19
DyHead [18]	ResNeXt-101-64x4d	test-dev	24	47.7	65.7	51.9	31.5	51.7	60.7	CVPR21
DW [51]	ResNeXt-101-64x4d	test-dev	24	48.2	67.1	52.2	29.6	51.2	60.8	CVPR22
TOOD [14]	ResNeXt-101-64x4d	test-dev	24	48.3	66.5	52.4	30.7	51.3	58.6	ICCV21
Deformable DETR [52]	ResNeXt-101-64x4d	test-dev	50	49.0	68.5	53.2	29.7	51.7	62.8	ICLR21
UniHead	ResNeXt-101-64x4d	test-dev	24	49.3	68.2	53.8	30.8	52.8	60.8	-
Mask R-CNN [53]	Swin-T	test-dev	36	46.0	68.1	50.3	31.2	49.2	60.1	ICCV17
ATSS [50]	Swin-T	test-dev	36	47.2	66.5	51.3	-	-	-	CVPR20
Sparse R-CNN [49]	Swin-T	test-dev	36	47.9	67.3	52.3	-	-	-	CVPR21
DyHead [18]	Swin-T	test-dev	24	49.7	68.0	54.3	33.3	54.2	64.2	CVPR21
RepPoints v2 [47]	Swin-T	test-dev	36	50.0	68.6	53.7	33.3	53.6	65.1	NeurIPS20
Mask RepPoints v2 [47]	Swin-T	test-dev	36	50.4	69.3	54.6	33.5	53.8	66.0	NeurIPS20
Cascade Mask R-CNN [28]	Swin-T	test-dev	36	50.4	69.2	54.7	33.8	54.1	65.2	CVPR18
UniHead	Swin-T	test-dev	36	51.3	70.1	56.1	32.5	54.5	64.3	-
UniHead	Swin-B †	test-dev	36	54.3	73.2	59.1	35.1	57.8	68.5	-

computations. These results illustrate the effectiveness and efficiency of our method.

Cooperating with Different Backbones. We demonstrate the compatibility of our approach with various backbones and compare it with state-of-the-art (SOTA) detectors. We leverage GFLv2 [48] as our detection framework with a number of perception modules of 1, 3, 3. We train 24 epochs for the CNN-based backbone and 36 epochs for the Transformer-based backbone. We adopt multi-scale training strategy during training and test our model on a single scale. For a fair comparison, we report the results of other models using multi-scale

training and single scale testing. As shown in Table II, Our UniHead achieves more dramatically impressive performance with potent backbones and surpasses the counterpart SOTA model by a large margin. Specifically, when compared to the best detector TOOD [14], with same settings, our method outperforms it by 1.0 AP with the ResNet-101 backbone. Compared with the advanced DETR series [35], [36], [52], our UniHead can achieve higher accuracy with fewer training epochs (24 epochs v.s. 50 epochs). Our UniHead is also compatible with Transformer-based backbone (Swin-T [21]) and outperforms excellent Cascade Mask R-CNN [28] by 0.9

TABLE III

ABLATION STUDY ON THE EFFECTIVENESS OF EACH PERCEPTION MODULE IN OUR UniHEAD. DP, GP, CTP REPRESENT DEFORMATION PERCEPTION, GLOBAL PERCEPTION AND CROSS-TASK PERCEPTION, RESPECTIVELY.

DP	GP	CTP	#Param.	FLOPs	AP	AP ₅₀	AP ₇₅
Baseline			37.74M	239.32G	36.5	55.4	39.1
✓	×	×	33.67M	152.60G	34.3	54.9	36.9
×	✓	×	34.54M	173.49G	35.8	56.8	38.0
×	×	✓	35.17M	190.41G	36.6	56.9	38.6
×	✓	✓	36.69M	225.21G	37.9	58.3	40.1
✓	×	✓	35.82M	204.32G	38.0	58.4	40.3
✓	✓	×	35.19M	187.40G	37.9	58.9	40.9
✓	✓	✓	37.34M	239.12G	39.2	59.7	41.7

TABLE IV

PERFORMANCE OF STACKING DIFFERENT NUMBERS OF PERCEPTION MODULES IN OUR UniHEAD.

DConv	DAT	CIT	#Param.	FLOPs	AP	AP ₅₀	AP ₇₅
Baseline			37.74M	239.32G	36.5	55.4	39.1
1	1	1	35.51M	195.86G	38.2	58.8	40.8
1	2	2	37.34M	239.12G	39.2	59.7	41.7
1	3	3	39.17M	282.38G	39.8	60.2	42.6
1	4	4	41.00M	325.64G	39.9	60.5	42.4

AP. Moreover, we use Swin-B [21] pre-trained on ImageNet-22K dataset [22] as the backbone to explore the performance improvements with large models. As shown in Table II, with a stronger backbone and pre-trained model, our UniHead achieves a tremendous performance improvement to 54.3 AP, demonstrating the potential for further improvements of our method.

D. Ablation Study

We perform detailed and comprehensive ablation studies to demonstrate the effectiveness and efficiency of our UniHead. For the ablation study, UniHead is applied to RetinaNet with ResNet-50 backbone and trained for 12 epochs without multi-scale training.

Effectiveness of Perception Modules. To evaluate the effectiveness of each proposed module, we conduct a controlled study in which we *eliminate* the parallel head used in RetinaNet and gradually add different perception modules to it. The results of the study are presented in Table III. Our findings indicate that when only one perception is applied to RetinaNet, it fails to achieve satisfactory results. Interestingly, we observe that the use of cross-task perception alone outperforms the baseline, underscoring the significance of cross-task interaction. With the addition of more perception modules, we observe an impressive enhancement in RetinaNet’s performance. For instance, when both global and cross-task perception are utilized, our UniHead surpasses the baseline by 1.4 AP, *even with much lower computational complexity*. Finally, our full UniHead that integrates three perceptual capabilities significantly improves the baseline by 2.7 AP.

Number of Perception Modules. We evaluate the efficiency and scalability of our method by stacking different

TABLE V

EFFECTIVENESS OF THE DEFORMATION PERCEPTION. CONV INDICATES 3×3 CONVOLUTION.

Method	#Param.	FLOPs	AP	AP ₅₀	AP ₇₅
Conv	37.28M	237.79G	38.8	59.1	42.1
DConv	37.34M	239.12G	39.2	59.7	41.7

TABLE VI

COMPARISON WITH OTHER TRANSFORMER MODULES.

Method	#Param.	FLOPs	AP	AP ₅₀	AP ₇₅
Swin Block [21]	37.40M	240.10G	38.8	59.3	41.4
CSwin Block [43]	37.40M	259.82G	38.9	59.6	41.3
Axial Attention [41]	37.40M	240.36G	38.9	59.4	41.7
DAT (Ours)	37.34M	239.12G	39.2	59.7	41.7

TABLE VII

ABLATION ON DIFFERENT STRIPE WIDTHS IN THE GLOBAL PERCEPTION MODULE.

Stripe width	#Param.	FLOPs	AP	AP ₅₀	AP ₇₅
1	37.34M	239.12G	39.2	59.7	41.7
3	37.34M	245.70G	38.9	59.4	41.4
5	37.34M	248.96G	38.8	59.3	41.6

numbers of perception modules. The deformation perception module can be regarded as an implicit position encoding [45], and therefore, we keep its number at 1. As indicated in Table IV, our method can consistently gain considerable performance improvements by stacking more modules until the numbers of modules reaches 1, 4, 4. Notably, even with much lower complexity, our method, which employs one module per perception type, can significantly outperform the baseline by 1.7 AP. It demonstrates the efficiency of our method. Moreover, when we adopt the model configuration of 1, 3, 3, the UniHead achieves 39.8 AP, which significantly improves the baseline by 3.3 AP, illustrating the powerfulness and scalability of our method.

Effectiveness of Deformation Perception Module. We evaluate the effectiveness of deformation perception by replacing the proposed DPM with a standard 3×3 convolution. As reported in Table V, the DPM outperforms the vanilla convolution by 0.4 AP. This suggests that the deformation perception introduced by DPM can boost the model’s representation ability and detection performance.

Comparison with other Transformer modules. We compare the proposed a Dual-axial Aggregation Transformer (DAT) with other classical Transformer modules, including Swin-Transformer block [21], CSwin-Transformer block [43] and axial attention [41]. We replace the DAT with these Transformer modules while maintaining the other structures unchanged for a fair comparison. The results are reported in Table VI. Obviously, our proposed DAT is superior to other Transformer modules in terms of efficiency and performance.

Stripe width. Table VII presents an ablation analysis of the stripe width in the global perception module. The results reveal that the expansion of the attention area does not lead



Fig. 5. Visualization of detection results of RetinaNet with parallel head and RetinaNet with UniHead. With our UniHead, the model is capable of more effectively detecting objects with diverse deformations and scales, and it can produce high-confidence precise bounding boxes. The major difference is marked by the orange circle. Zoom in for a better view.

TABLE VIII
THE EFFECT OF THE CROSS-AXIS AGGREGATION BLOCK (CAB) IN THE GLOBAL PERCEPTION MODULE.

CAB	#Param.	FLOPs	AP	AP ₅₀	AP ₇₅
	37.34M	239.01G	39.0	59.7	41.5
✓	37.34M	239.12G	39.2	59.7	41.7

TABLE IX
EFFECTIVENESS OF THE CROSS-TASK INTERACTION.

Method	#Param.	FLOPs	AP	AP ₅₀	AP ₇₅
CSA	37.34M	239.12G	38.9	59.7	41.4
CCA	37.34M	239.12G	39.2	59.7	41.7

to further improvements in the model’s performance; in fact, it may even cause a decline in its performance. This indicates that the potency of the DAT is derived from its efficient parallel structure, which allows the model perceive global information.

Effectiveness of the Cross-axis Aggregation Block. In Table VIII, we present the results of employing the cross-axis aggregation block (CAB) in our approach. CAB effectively integrates both local and cross-axis information for horizontal and vertical axial attention, thus gaining performance improvement.

Effectiveness of the Cross-Task Perception. To evaluate the effect of cross-task perception, we replace the proposed cross-task channel-wise attention (CCA) with channel-wise self-attention (CSA), and the results are presented in Table IX. The results demonstrate that our proposed CCA outperforms the CSA by 0.3 AP, without adding additional parameters and computations. This indicates that incorporating cross-task information can effectively guide feature learning for

TABLE X
THE EFFECT OF THE LOCALITY ENHANCEMENT BLOCK (LEB) IN THE CROSS-TASK PERCEPTION MODULE.

LEB	#Param.	FLOPs	AP	AP ₅₀	AP ₇₅
	37.31M	238.46G	39.0	59.5	41.8
✓	37.34M	239.12G	39.2	59.7	41.7

TABLE XI
APPLYING UNIHEAD TO TWO-STAGE MODELS FOR OBJECT DETECTION (BBOX) AND INSTANCE SEGMENTATION (SEGM).

Detector	Note	Task	AP	AP ₅₀	AP ₇₅
Faster R-CNN [27]	baseline	BBox	37.4	58.1	40.4
Faster R-CNN [27]	UniHead	BBox	39.0	59.7	42.5
Mask R-CNN [53]	baseline	Segm	34.7	55.7	37.2
Mask R-CNN [53]	UniHead	Segm	35.8	56.6	38.3

classification and localization tasks, thus achieving higher performance.

Effectiveness of Locality Enhancement Block. We ablate the locality enhancement block (LEB) in the cross-task perception module. As shown in Table X, the proposed LEB is lightweight and improves the model by 0.2 AP, proving the significance of the locality enhancement.

E. Visualization

We visualize the detection results using RetinaNet and after replacing its parallel head with UniHead. As shown in Fig. 5, UniHead can detect objects in complex scenes more effectively, where the objects have various scales and diverse geometric transformations. Notably, the third column of the figure highlights UniHead’s proficiency in detecting small objects effectively. This excellent detection performance,

particularly for complex-shaped and small objects, underscores the efficacy of deformation perception and global perception. Furthermore, as depicted in the last column of Fig. 5, our method can provide precise detection boxes with higher classification scores, indicating that UniHead can help the detector output more consistent results in both classification and localization.

F. Further Generalization Verification

We further generalize our UniHead to representative two-stage models on two scenes, including object detection using Faster R-CNN [27] and instance segmentation using Mask R-CNN [53]. Although two-stage models does not have the parallel head, our UniHead can be easily integrated into them. We use our UniHead to replace the convolution before performing proposal prediction in the Region Proposal Network (RPN). Note the convolution number in RPN is one, so UniHead is used after channel reduction to avoid increasing much complexity. As shown in Table XI, our model still achieves very stunning performance on these scenarios. Specifically, the UniHead improves Faster R-CNN by 1.6 AP and Mask R-CNN by 1.1 AP, fully validating the generalization ability of our approach.

V. CONCLUSION

In this paper, we propose UniHead, a novel approach that unifies deformation perception, global perception, and cross-task perception in a single head. Firstly, we introduce the deformation perception, which allows the model to adaptively sample the features of objects. Secondly, we design an innovative Dual-axial Aggregation Transformer (DAT) to learn global features effectively. Lastly, we develop the Cross-task Interaction Transformer (CIT), which enables interaction between classification and localization tasks to promote the alignment of the two tasks. As a plugin block, our UniHead can be flexibly integrated into existing object detectors and significantly enhance their performance without adding any model complexity.

REFERENCES

- [1] K. He, X. Zhang, S. Ren, and J. Sun, "Deep residual learning for image recognition," in *Proceedings of the IEEE conference on computer vision and pattern recognition*, 2016, pp. 770–778.
- [2] C.-Y. Wang, H.-Y. M. Liao, Y.-H. Wu, P.-Y. Chen, J.-W. Hsieh, and I.-H. Yeh, "Cspnet: A new backbone that can enhance learning capability of cnn," in *Proceedings of the IEEE conference on computer vision and pattern recognition workshops*, 2020, pp. 390–391.
- [3] M. Tan, R. Pang, and Q. V. Le, "Efficientdet: Scalable and efficient object detection," in *Proceedings of the IEEE conference on computer vision and pattern recognition*, 2020, pp. 10 781–10 790.
- [4] T.-Y. Lin, P. Dollár, R. Girshick, K. He, B. Hariharan, and S. Belongie, "Feature pyramid networks for object detection," in *Proceedings of the IEEE conference on computer vision and pattern recognition*, 2017, pp. 2117–2125.
- [5] S. Liu, L. Qi, H. Qin, J. Shi, and J. Jia, "Path aggregation network for instance segmentation," in *Proceedings of the IEEE conference on computer vision and pattern recognition*, 2018, pp. 8759–8768.
- [6] G. Ghiasi, T.-Y. Lin, and Q. V. Le, "Nas-fpn: Learning scalable feature pyramid architecture for object detection," in *Proceedings of the IEEE conference on computer vision and pattern recognition*, 2019, pp. 7036–7045.
- [7] T.-Y. Lin, P. Goyal, R. Girshick, K. He, and P. Dollár, "Focal loss for dense object detection," in *Proceedings of the IEEE international conference on computer vision*, 2017, pp. 2980–2988.
- [8] X. Li, W. Wang, L. Wu, S. Chen, X. Hu, J. Li, J. Tang, and J. Yang, "Generalized focal loss: Learning qualified and distributed bounding boxes for dense object detection," *Advances in Neural Information Processing Systems*, vol. 33, pp. 21 002–21 012, 2020.
- [9] S. Zhang, C. Chi, Y. Yao, Z. Lei, and S. Z. Li, "Bridging the gap between anchor-based and anchor-free detection via adaptive training sample selection," in *Proceedings of the IEEE conference on computer vision and pattern recognition*, 2020, pp. 9759–9768.
- [10] Z. Ge, S. Liu, Z. Li, O. Yoshie, and J. Sun, "Ota: Optimal transport assignment for object detection," in *Proceedings of the IEEE Conference on Computer Vision and Pattern Recognition*, 2021, pp. 303–312.
- [11] J. Cao, Y. Pang, J. Han, and X. Li, "Hierarchical regression and classification for accurate object detection," *IEEE Transactions on Neural Networks and Learning Systems*, 2021.
- [12] M. Mao, Y. Tian, B. Zhang, Q. Ye, W. Liu, and D. Doermann, "Iffdetector: inference-aware feature filtering for object detection," *IEEE Transactions on Neural Networks and Learning Systems*, vol. 33, no. 11, pp. 6494–6503, 2021.
- [13] Z. Tian, C. Shen, H. Chen, and T. He, "Fcos: Fully convolutional one-stage object detection," in *Proceedings of the IEEE international conference on computer vision*, 2019, pp. 9627–9636.
- [14] C. Feng, Y. Zhong, Y. Gao, M. R. Scott, and W. Huang, "Tood: Task-aligned one-stage object detection," in *Proceedings of the IEEE international conference on computer vision*, 2021, pp. 3490–3499.
- [15] Y. Wu, Y. Chen, L. Yuan, Z. Liu, L. Wang, H. Li, and Y. Fu, "Rethinking classification and localization for object detection," in *Proceedings of the IEEE conference on computer vision and pattern recognition*, 2020, pp. 10 186–10 195.
- [16] Z. Yang, S. Liu, H. Hu, L. Wang, and S. Lin, "Reppoints: Point set representation for object detection," in *Proceedings of the IEEE international conference on computer vision*, 2019, pp. 9657–9666.
- [17] X. Zhang, F. Wan, C. Liu, R. Ji, and Q. Ye, "Freeanchor: Learning to match anchors for visual object detection," *Advances in neural information processing systems*, vol. 32, 2019.
- [18] X. Dai, Y. Chen, B. Xiao, D. Chen, M. Liu, L. Yuan, and L. Zhang, "Dynamic head: Unifying object detection heads with attentions," in *Proceedings of the IEEE conference on computer vision and pattern recognition*, 2021, pp. 7373–7382.
- [19] J. Dai, H. Qi, Y. Xiong, Y. Li, G. Zhang, H. Hu, and Y. Wei, "Deformable convolutional networks," in *Proceedings of the IEEE international conference on computer vision*, 2017, pp. 764–773.
- [20] T.-Y. Lin, M. Maire, S. Belongie, J. Hays, P. Perona, D. Ramanan, P. Dollár, and C. L. Zitnick, "Microsoft coco: Common objects in context," in *Computer Vision—ECCV 2014: 13th European Conference, Zurich, Switzerland, September 6–12, 2014, Proceedings, Part V 13*. Springer, 2014, pp. 740–755.
- [21] Z. Liu, Y. Lin, Y. Cao, H. Hu, Y. Wei, Z. Zhang, S. Lin, and B. Guo, "Swin transformer: Hierarchical vision transformer using shifted windows," in *Proceedings of the IEEE international conference on computer vision*, 2021, pp. 10 012–10 022.
- [22] J. Deng, W. Dong, R. Socher, L.-J. Li, K. Li, and L. Fei-Fei, "Imagenet: A large-scale hierarchical image database," in *2009 IEEE conference on computer vision and pattern recognition*. Ieee, 2009, pp. 248–255.
- [23] Z.-Q. Zhao, P. Zheng, S.-t. Xu, and X. Wu, "Object detection with deep learning: A review," *IEEE transactions on neural networks and learning systems*, vol. 30, no. 11, pp. 3212–3232, 2019.
- [24] K.-H. Shih, C.-T. Chiu, J.-A. Lin, and Y.-Y. Bu, "Real-time object detection with reduced region proposal network via multi-feature concatenation," *IEEE transactions on neural networks and learning systems*, vol. 31, no. 6, pp. 2164–2173, 2019.
- [25] R. Girshick, J. Donahue, T. Darrell, and J. Malik, "Rich feature hierarchies for accurate object detection and semantic segmentation," in *Proceedings of the IEEE conference on computer vision and pattern recognition*, 2014, pp. 580–587.
- [26] R. Girshick, "Fast r-cnn," in *Proceedings of the IEEE international conference on computer vision*, 2015, pp. 1440–1448.
- [27] S. Ren, K. He, R. Girshick, and J. Sun, "Faster r-cnn: Towards real-time object detection with region proposal networks," *Advances in neural information processing systems*, vol. 28, 2015.
- [28] Z. Cai and N. Vasconcelos, "Cascade r-cnn: Delving into high quality object detection," in *Proceedings of the IEEE conference on computer vision and pattern recognition*, 2018, pp. 6154–6162.

- [29] J. Hu, L. Shen, and G. Sun, "Squeeze-and-excitation networks," in *Proceedings of the IEEE conference on computer vision and pattern recognition*, 2018, pp. 7132–7141.
- [30] R. Yang, L. Song, Y. Ge, and X. Li, "Boxsnake: Polygonal instance segmentation with box supervision," *arXiv preprint arXiv:2303.11630*, 2023.
- [31] H. Zhou, R. Yang, R. Hu, C. Shu, X. Tang, and X. Li, "Etdnet: Efficient transformer-based detection network for surface defect detection," *IEEE Transactions on Instrumentation and Measurement*, 2023.
- [32] G. Xu, C. He, H. Wang, H. Zhu, and W. Ding, "Dm-fusion: Deep model-driven network for heterogeneous image fusion," *IEEE Transactions on Neural Networks and Learning Systems*, 2023.
- [33] A. Dosovitskiy, L. Beyer, A. Kolesnikov, D. Weissenborn, X. Zhai, T. Unterthiner, M. Dehghani, M. Minderer, G. Heigold, S. Gelly *et al.*, "An image is worth 16x16 words: Transformers for image recognition at scale," *arXiv preprint arXiv:2010.11929*, 2020.
- [34] R. Yang, H. Ma, J. Wu, Y. Tang, X. Xiao, M. Zheng, and X. Li, "Scalablevit: Rethinking the context-oriented generalization of vision transformer," in *Computer Vision–ECCV 2022: 17th European Conference, Tel Aviv, Israel, October 23–27, 2022, Proceedings, Part XXIV*. Springer, 2022, pp. 480–496.
- [35] F. Li, H. Zhang, S. Liu, J. Guo, L. M. Ni, and L. Zhang, "Dn-detr: Accelerate detr training by introducing query denoising," in *Proceedings of the IEEE Conference on Computer Vision and Pattern Recognition*, 2022, pp. 13 619–13 627.
- [36] S. Liu, F. Li, H. Zhang, X. Yang, X. Qi, H. Su, J. Zhu, and L. Zhang, "Dab-detr: Dynamic anchor boxes are better queries for detr," *arXiv preprint arXiv:2201.12329*, 2022.
- [37] A. Hatamizadeh, H. Yin, J. Kautz, and P. Molchanov, "Global context vision transformers," *arXiv preprint arXiv:2206.09959*, 2022.
- [38] T. Huang, L. Huang, S. You, F. Wang, C. Qian, and C. Xu, "Lightvit: Towards light-weight convolution-free vision transformers," *arXiv preprint arXiv:2207.05557*, 2022.
- [39] W. Wang, E. Xie, X. Li, D.-P. Fan, K. Song, D. Liang, T. Lu, P. Luo, and L. Shao, "Pyramid vision transformer: A versatile backbone for dense prediction without convolutions," in *Proceedings of the IEEE international conference on computer vision*, 2021, pp. 568–578.
- [40] —, "Pvt v2: Improved baselines with pyramid vision transformer," *Computational Visual Media*, vol. 8, no. 3, pp. 415–424, 2022.
- [41] J. Ho, N. Kalchbrenner, D. Weissenborn, and T. Salimans, "Axial attention in multidimensional transformers," *arXiv preprint arXiv:1912.12180*, 2019.
- [42] Z. Huang, X. Wang, L. Huang, C. Huang, Y. Wei, and W. Liu, "Ccnets: Criss-cross attention for semantic segmentation," in *Proceedings of the IEEE international conference on computer vision*, 2019, pp. 603–612.
- [43] X. Dong, J. Bao, D. Chen, W. Zhang, N. Yu, L. Yuan, D. Chen, and B. Guo, "Cswin transformer: A general vision transformer backbone with cross-shaped windows," in *Proceedings of the IEEE Conference on Computer Vision and Pattern Recognition*, 2022, pp. 12 124–12 134.
- [44] X. Zhu, H. Hu, S. Lin, and J. Dai, "Deformable convnets v2: More deformable, better results," in *Proceedings of the IEEE conference on computer vision and pattern recognition*, 2019, pp. 9308–9316.
- [45] X. Chu, Z. Tian, B. Zhang, X. Wang, X. Wei, H. Xia, and C. Shen, "Conditional positional encodings for vision transformers," *arXiv preprint arXiv:2102.10882*, 2021.
- [46] K. Chen, J. Wang, J. Pang, Y. Cao, Y. Xiong, X. Li, S. Sun, W. Feng, Z. Liu, J. Xu *et al.*, "Mmdetection: Open mmlab detection toolbox and benchmark," *arXiv preprint arXiv:1906.07155*, 2019.
- [47] Y. Chen, Z. Zhang, Y. Cao, L. Wang, S. Lin, and H. Hu, "Reppoints v2: Verification meets regression for object detection," *Advances in Neural Information Processing Systems*, vol. 33, pp. 5621–5631, 2020.
- [48] X. Li, W. Wang, X. Hu, J. Li, J. Tang, and J. Yang, "Generalized focal loss v2: Learning reliable localization quality estimation for dense object detection," in *Proceedings of the IEEE Conference on Computer Vision and Pattern Recognition*, 2021, pp. 11 632–11 641.
- [49] P. Sun, R. Zhang, Y. Jiang, T. Kong, C. Xu, W. Zhan, M. Tomizuka, L. Li, Z. Yuan, C. Wang *et al.*, "Sparse r-cnn: End-to-end object detection with learnable proposals," in *Proceedings of the IEEE conference on computer vision and pattern recognition*, 2021, pp. 14 454–14 463.
- [50] K. Chen, J. Pang, J. Wang, Y. Xiong, X. Li, S. Sun, W. Feng, Z. Liu, J. Shi, W. Ouyang *et al.*, "Hybrid task cascade for instance segmentation," in *Proceedings of the IEEE conference on computer vision and pattern recognition*, 2019, pp. 4974–4983.
- [51] S. Li, C. He, R. Li, and L. Zhang, "A dual weighting label assignment scheme for object detection," in *Proceedings of the IEEE Conference on Computer Vision and Pattern Recognition*, 2022, pp. 9387–9396.
- [52] X. Zhu, W. Su, L. Lu, B. Li, X. Wang, and J. Dai, "Deformable detr: Deformable transformers for end-to-end object detection," *arXiv preprint arXiv:2010.04159*, 2020.
- [53] K. He, G. Gkioxari, P. Dollár, and R. Girshick, "Mask r-cnn," in *Proceedings of the IEEE international conference on computer vision*, 2017, pp. 2961–2969.